J Neurophysiol 99: 1493–1502, 2008.
First published January 16, 2008; doi:10.1152/jn.00959.2007.

Behavioral and Physiological Characterization of Sensorimotor Gating in the Goldfish Startle Response

Heike Neumeister, Theresa M. Szabo, and Thomas Preuss
Dominick Purpura Department of Neuroscience, Albert Einstein College of Medicine, Bronx, New York

Submitted 25 August 2007; accepted in final form 12 January 2008

Neumeister H, Szabo TM, Preuss T. Behavioral and physiological characterization of sensorimotor gating in the goldfish startle response. *J Neurophysiol* 99: 1493–1502, 2008. First published January 16, 2008; doi:10.1152/jn.00959.2007. Prepulse inhibition (PPI) is typically associated with an attenuation of auditory startle behavior in mammals and is presumably mediated within the brainstem startle circuit. However, the inhibitory mechanisms underlying PPI are not yet clear. We addressed this question with complementary behavioral and in vivo electrophysiological experiments in the startle escape circuit of goldfish, the Mauthner cell (M-cell) system. In the behavioral experiments we observed a 77.5% attenuation (PPI) of startle escape probability following auditory prepulse–pulse stimulation. The PPI effect was observed for prepulse–pulse interstimulus intervals (ISIs) ranging from 20 to 600 ms and its magnitude depended linearly on prepulse intensity over a range of 14 dB. Electrophysiological recordings of synaptic responses to a sound pulse in the M-cell, which is the sensorimotor neuron initiating startle escapes, showed a 21% reduction in amplitude of the dendritic postsynaptic potential (PSP) and a 23% reduction of the somatic PSP following a prepulse. In addition, a prepulse evoked a long-lasting (500 ms) decrease in M-cell excitability indicated by *1*) an increased threshold current, *2*) an inhibitory shunt of the action potential (AP), and *3*) by a linearized M-cell membrane, which effectively impedes M-cell AP generation. Comparing the magnitude and kinetics of inhibitory shunts evoked by a prepulse in the M-cell dendrite and soma revealed a disproportionately larger and longer-lasting inhibition in the dendrite. These results suggest that the observed PPI-type attenuation of startle behavior can be correlated to distinct postsynaptic mechanisms mediated primarily at the M-cell lateral dendrite.

INTRODUCTION

Startle, a fast behavioral response to a sudden stimulus, has common characteristics in many animals (Eaton 1984; Koch 1999). In vertebrates, auditory startle is mediated by lower brain stem circuits characterized by large neurons that receive direct afferent input and, in turn, activate vast numbers of spinal motor neurons within 4–15 ms (Davis et al. 1982; Eaton et al. 1991; Koch 1999; Korn and Faber 1996; Lee et al. 1996; Yeomans and Frankland 1996). Despite its reflexive nature, the startle response shows plasticity at many levels. One such example, prepulse inhibition (PPI), is typically associated with a sensory-evoked attenuation of the auditory startle response in rats (whole-body flinch) and humans (eye blink reflex) and serves as an important research and diagnostic tool for several cognitive and information processing disorders (reviewed in Braff et al. 2001; Grillon and Baas 2003; Swerdlow and Geyer 1998; Swerdlow et al. 2001). Experimentally, PPI is produced when a startling stimulus (pulse) is preceded within 20–500 ms by a nonstartling stimulus (prepulse) of the same or another modality (Graham 1975; Hoffman and Ison 1980). Electrophysiology experiments in mammals suggest the inhibitory effects of a prepulse are mediated within the elementary startle circuit in the brain stem (Bosch and Schmid 2006; Carlson and Willott 1998; Fendt and Yeomans 2001; Lingenhöhl and Friauf 1992, 1994). However, the inhibitory mechanisms underlying motor output attenuation during PPI in vertebrates are not yet clear.

Recent studies of PPI in a marine mollusk emphasize the role of pre- and postsynaptic inhibition in suppressing sensory inputs and modulating the flow of information to downstream motor circuits (Frost et al. 2003; Mongeluzi et al. 1998). Thus it is important to ask whether similar or different mechanisms underlie PPI in a vertebrate startle circuit, using a model system that is accessible for in vivo electrophysiology and exhibits PPI in a manner similar to that seen in mammals. For this purpose we use the Mauthner cell (M-cell) system of goldfish, which mediates a short-latency startle behavior in response to auditory stimuli (Eaton et al. 1991; Faber et al. 1989; Preuss and Faber 2003; Weiss et al. 2006; Zottoli 1977). The M-cells are a bilateral pair of large reticulospinal neurons processing multimodal information. A single action potential (AP) in one M-cell reliably activates contralateral spinal motor networks, causing a fast C-shaped body bend (C-start) away from the side of the excited M-cell (Eaton et al. 1981; Zottoli 1977; reviewed in Korn and Faber 2005). In addition, PPI has recently been shown to attenuate C-start escape behavior in zebrafish (Burgess and Granato 2007).

In the present study, we demonstrate a PPI-type attenuation during auditory-evoked startle escapes in free-swimming adult goldfish. Our electrophysiological results demonstrate a corresponding reduction in M-cell excitability and this attenuation involves the recruitment of postsynaptic mechanisms.

METHODS

Animals

Goldfish (*Carassius auratus*), 7–10 cm in body length, were purchased from EECHO Systems (North Kansas City, MO), Hunting Creek Fisheries (Thurmond, MD), or Billy Bland Fisheries (Taylor, AR). They were acclimated to our holding system for at least 1 mo, allowing recovery from stress associated with transportation and adjustment to laboratory conditions. Fish were housed in groups of 10–15 in a 120-liter holding tank system, containing recirculating conditioned water at 18°C, and were exposed to a 12/12-h light/dark photoperiodic cycle. Details for water conditioning have been de-

Address for reprint requests and other correspondence: T. Preuss, Dominick Purpura Department of Neuroscience, Albert Einstein College of Medicine, 1300 Morris Park Ave., Bronx, NY 10461 (E-mail: tpreuss@aecom.yu.edu).

The costs of publication of this article were defrayed in part by the payment of page charges. The article must therefore be hereby marked "*advertisement*" in accordance with 18 U.S.C. Section 1734 solely to indicate this fact.

scribed previously (Szabo et al. 2006). Water quality was monitored regularly and was the same for holding and experimental tanks (pH 7.2 ± 0.2; dissolved oxygen saturated, 8 pp).

Behavioral setup and stimulation

Startle experiments were conducted in a circular acrylic tank (diameter: 76 cm; water height: 6–20 cm) supplied from a water reservoir attached to a chiller (Delta Star, AquaLogic, Apopka, FL) for maintaining 18 ± 1°C water temperature. The tank was mounted onto an antivibration table to eliminate external mechanosensory cues and opaque covers and a curtain surrounding the tank eliminated external visual cues. By use of a small plastic container fish were transferred from the holding tank into the experimental tank and acclimation time prior to experimental trials was 30–40 min. Experiments were conducted using one fish at a time and typically lasted 2.5 h.

Ventral views of freely swimming fish were recorded via a mirror placed below the tank at a 45° angle, using two high-speed color video cameras (resolution 512 × 384 pixels; 1,000 frames/s; Kodak Extapro 1000 HRC, Eastman Kodak, San Diego, CA). Data acquired with the high-speed cameras, typically 1 s per trial, were stored on a DV tape or DVD.

Sound stimuli were produced alternately by two underwater loudspeakers (UW-30; University Sound, Buchanan, MI) on opposite sites and supported within a 6-cm-thick layer of foam lining the entire inner wall of the tank. Auditory prepulse and pulse (startle) stimuli consisted of brief (5-ms) 200-Hz sound pips, created as single-cycle sine waves in Igor Pro (WaveMetrics, Portland, OR) and amplified with a Servo 120 amplifier (Samson, Soysset, NY). The prepulse stimulus ranged in intensity from 128 to 144 dB with a reference (re) value of 1 micropascal (μPa) in water (which translates to 66.5–82 dB re 20 μPa in air) and typically did not evoke a startle response. Trials in which the prepulse evoked a startle were excluded from the data analysis. The startling pulse stimulus ranged in intensity between 159 and 169 dB re 1 μPa in water.

Stimulus onset was marked on the high-speed video image by a light-emitting diode mounted in the optical path outside of the tank; the fish did not see this marker. In addition, the waveform and amplitude of the auditory stimuli were recorded using SQ01 hydrophones (Sensor Technology, Collingwood, Ontario, Canada) located at the tank wall near and between the loudspeakers.

Behavioral experiments

The rationale of the behavioral experiments was to determine whether a nonstartling auditory prepulse immediately preceding a startling auditory pulse stimulus modifies startle escape behavior, specifically escape probability and latency. These two measures have been shown to depend directly on M-cell activity; i.e., lesion of the M-cells decreases the probability of a C-start occurring and increases C-start latency (Liu and Fetcho 1999; Zottoli et al. 1999).

An experiment typically started with five pulse stimuli (without prepulse) to assess the baseline escape probability of an individual. This was followed by 20–40 prepulse–pulse combination trials intermixed with pulse control trials. Intertrial intervals varied pseudorandomly within a range of 0.5–30 min (mean 3.5 min) to avoid possible habituation effects. Similarly, prepulse and pulse stimulus intensities and ISIs between prepulse and pulse were delivered in a pseudorandom order throughout the experiment.

Electrophysiology

These experiments involved standard in vivo surgical and recording techniques used previously (Preuss and Faber 2003). Goldfish were initially anesthetized by immersion in 1°C water. A topical anesthetic (20% benzocaine gel; Ultradent) was then applied at the incision site on the skin and the dorsal cranium for 5 min before dissection. The fish was stabilized in the recording chamber by two pins, one on each side of the head, further immobilized with intramuscular injections of *d*-tubocurarine (1–3 μg/g body weight), and respirated through the mouth with a steady flow of aerated saline containing the general anesthetic MS-222 at a concentration of 20 mg/l. This concentration has been shown to have little if any effect on the spontaneous activity and mechanosensory responses of peripheral sensory nerves in fish (Palmer and Mensinger 2004). The recording chamber was mounted inside an opaque, thin-walled tank filled with temperature-controlled (18°C) saline covering the fish eyes.

A small lateral incision at the caudal midbody was made for exposure of the spinal cord. Bipolar electrodes were placed on the unopened spinal cord for antidromic activation of the M-axons with small pulses (5–8 V) using an isolated stimulator (Digitimer, Welwyn Garden City, UK). Antidromic stimulation fires the M-cell and produces a negative potential in the M-cell axon cap (typically 15–20 mV), thereby unambiguously identifying the location of the axon hillock and allowing intracellular recordings from the M-cell soma or along the lateral dendrite at defined locations (Faber et al. 1978; Furukawa 1966). A small hole was made in the cranium to expose the medulla for M-cell recordings.

Single or dual simultaneous intracellular recordings were made using an Axoprobe-1A amplifier (Axon Instruments, Foster City, CA) in current clamp with sharp electrodes filled with 5 M KAc (7–10 MΩ). The M-cell was stimulated orthodromically using 200-Hz sound pips (5 ms) with intensities ranging from 128 to 147 dB in water re 1 μPa produced by a subwoofer (SA-WN250; Sony). Sound stimuli were recorded with a microphone positioned above the fish, with a hydrophone inside the tank, and stored on-line together with the intracellular recordings.

The sound stimuli used for the electrophysiological experiments were designed to resemble those used in the behavioral experiments. However, several experimentally related limitations had to be considered.

First, goldfish detect both sound wave components: sound pressure and particle motion (Fay 1984; Furukawa and Ishii 1967; Popper and Fay 1999). The pressure component produces volume changes in the gas-filled swim bladder that are eventually detected by otolith end organs in both ears and provide a major sensory input to the M-cell (Casagrand et al. 1999; Furukawa 1966; Szabo et al. 2006, 2007). This component is likely not affected by fixation of the animal head with pins in the recording chamber.

The particle motion component, on the other hand, produces a net displacement of the fish, which is presumably also sensed by otolith organs and has been shown to provide input to the M-cell (Casagrand et al. 1999; Szabo et al. 2007). However, it is reasonable to assume that fixation of the animal effectively reduces or even eliminates the motion component of the underwater sound stimulus presented in the behavioral experiments.

Second, underwater loudspeakers could not be used because of the electronic noise they produced. Therefore a subwoofer was positioned outside the recording tank for sound production. The indirect sound transmission through the tank wall limited the maximum underwater sound intensity that could be produced to 147 dB in water re 1 μPa, which was 22 dB less than the maximum pulse stimulus in the behavioral setup. In other words, the sound intensities that reliably evoke escapes could not be achieved, but we could match the intensity range of the prepulse stimuli used in the behavioral experiments and study their influence on the M-cell system.

The effect of prepulse stimuli on M-cell membrane properties such as input resistance and threshold was determined with intracellular stimulation using a current ramp produced by a function generator (Wavetek 39, Norwich, UK) fed into the current command input of the Axoprobe amplifier and injected into the M-cell via an intrasomatic electrode while recording voltage with a second somatic or proximal dendritic electrode. Electrode cross talk was minimized electrically by an active circuit built into the Axoprobe amplifier.

Data were recorded on-line with a Macintosh G4, using a data acquisition card (PCI E, National Instruments Austin, TX) and acquisition software developed in the laboratory (sampling rate, 30–60 μs/point) and analyzed with the same software and with Igor Pro. Only one M-cell was recorded and analyzed in each animal for the physiology experiments.

Behavioral and electrophysiological experiments were performed in accordance with relevant guidelines and regulations of the Animal Institute Committee of the Albert Einstein College of Medicine.

Data analysis and statistics

Mean startle probabilities were calculated from the number of C-starts occurring within a given number of control or PPI trials for each animal and these two conditions were compared with paired-*t*-test.

The dependence of the PPI effect [formula: PPI effect = 100 − (escape probability with prepulse–pulse/escape probability with pulse) × 100; Zhang et al. 2000] on several ISIs was tested using a single-factor ANOVA.

Response latency, defined as the first detectable movement of the head after stimulus onset, was measured manually in successive video images as described previously (Preuss and Faber 2003).

Electrophysiological measurements were made on averaged sweeps (10–15) using custom software, or Igor Pro (WaveMetrics). Each experiment included control and prepulse trials and these two conditions were compared with paired-*t*-test unless otherwise noted.

All data are reported as means ± SE. N_A, N_T, and N_R denote the total number of animals, trials, and responses used for data analysis, respectively. Note: Because all experiments were performed underwater, sound intensities in the text and figures are reported as the sound pressure level (SPL) in water relative to 1 μPa, which translates to about 62 dB less in air relative to 20 μPa, i.e., relative to the human hearing threshold.

RESULTS

Effect of auditory prepulse on startle behavior

In all, 17 animals were used in the behavioral experiments. C-starts in response to single sound-pip stimuli were characterized by a short-latency C-shaped body bend (Fig. 1*A*) typical for M-cell–mediated startle escapes (Eaton et al. 1981; Weiss et al. 2006; Zottoli 1977). C-start probability depended on the intensity of the stimulus (Fig. 1*B*). Specifically, low-intensity sound pips ranging from 128 to 144 dB were associated with a low mean startle probability of 0.1 ± 0.02 (N_A = 17, N_T = 244); i.e., they were essentially subthreshold. In contrast, sounds pips ranging in intensity from 159 to 169 dB evoked C-starts with a mean probability of 0.74 ± 0.04 (N_A = 17, N_T = 98). Indeed, these two intensity ranges represent the lower and upper portions of a sigmoid-shaped stimulus–response relationship and they defined the respective strengths for prepulse and pulse stimuli for the behavioral tests.

Combined prepulse–pulse stimulation with a fixed interstimulus interval (ISI) of 50 ms resulted in a significant 77.5% reduction of C-start probability compared with control pulse stimuli alone ($P < 0.0001$; N_A = 12; Fig. 2*A*). All animals tested showed an attenuation of C-start probability in the range of 40–100%. Moreover, 9 of 12 animals were nonresponsive during the first prepulse–pulse combination trial, suggesting that, as in mammalian PPI, learning or habituation is presumably not involved in this phenomenon (Graham 1975).

As noted earlier, various prepulse intensities were used in the prepulse–pulse stimulation trials. However, the sound intensity for a given stimulus varied within the tank by about 4 dB; i.e., intensity decreased with increasing distance from the underwater loudspeaker. Thus to ensure a defined stimulus intensity we analyzed C-starts of trials with the animal at a distinct location only: in the center of the experimental tank. For these cases, escape probability in prepulse–pulse trials was inversely correlated to prepulse intensities (R^2 = 0.82; Fig. 2*B*).

The influence of ISI on PPI was tested by calculating the PPI effect (see METHODS) for four ISIs in trials with prepulse intensities ranging from 128 to 137 dB. This analysis included only lower prepulse intensities to avoid a possible PPI ceiling effect, which might mask the dependence of PPI on ISI. The results showed a maximum PPI effect at ISI 50 and a small decrease for longer ISIs (Fig. 2*C*). However, no significant differences for the PPI effect were found between the different ISIs (P = 0.83, ANOVA).

A comparison of escape latencies between C-starts evoked by pulse stimuli (N_A = 17, N_R = 101) and the few C-starts that occurred in response to prepulse–pulse combination stimuli (N_A = 17, N_R = 38; includes all prepulse intensities and ISIs trials) showed no significant difference (P = 0.5, unpaired *t*-test) with mean values of 13.6 ± 0.2 and 13.9 ± 0.5 ms, respectively. These short latencies suggest C-starts were initiated by the M-cell in both cases.

Effects of prepulse stimuli on sensory-evoked synaptic responses

To identify and characterize the physiological correlates of the observed behavioral attenuation produced by a prepulse we

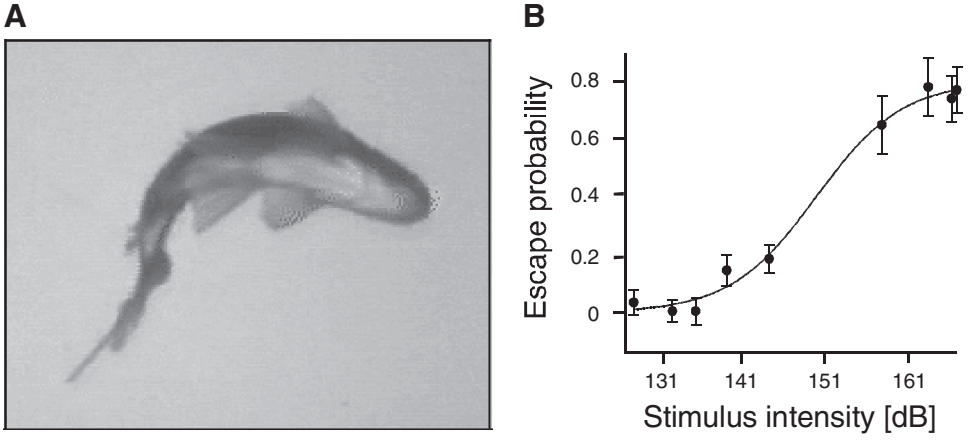

FIG. 1. Auditory startle behavior (C-start). *A*: video image of a goldfish filmed from below 41 ms after a sound pip, showing the typical C-body bend (stage 1) associated with contralateral Mauthner cell (M-cell) activation. *B*: scatterplot of mean escape probability vs. pip intensity fitted with a sigmoid function in Igor Pro [number of animals (N_A) = 17].

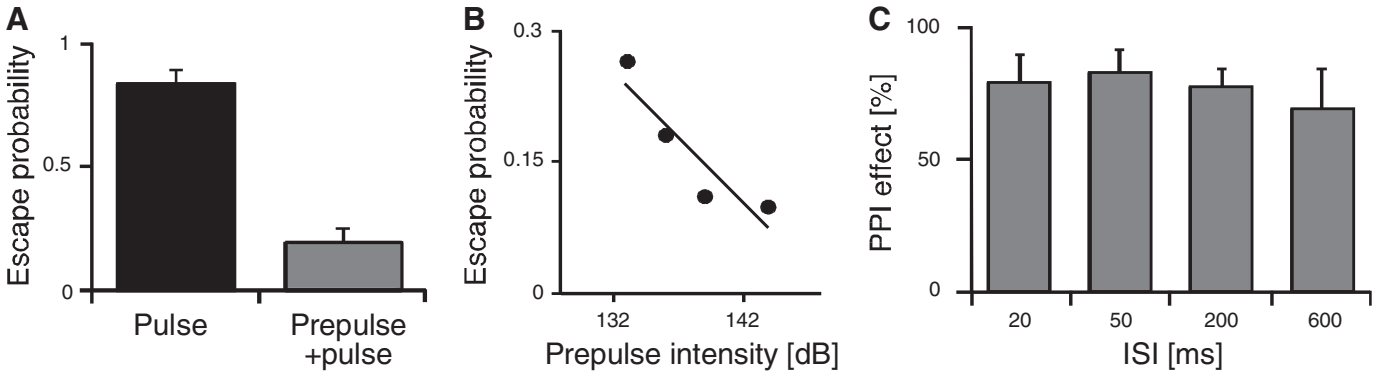

FIG. 2. Behavioral characteristics of prepulse inhibition (PPI). *A*: mean escape probability without (black) and with (gray) preceding prepulse (N_A = 12). *B*: influence of prepulse intensity on PPI. Plot of mean escape probabilities of prepulse–pulse trials only vs. prepulse intensity fitted with a linear function. From *left* to *right*, the points represent data from 6, 3, 4, and 5 fish, respectively. *C*: PPI effect over a range of interstimulus intervals (ISIs). Bar plots show mean PPI effect for indicated ISI times (N_A = 7).

performed a series of in vivo electrophysiological experiments (N_A = 15) in which we recorded intracellularly from the M-cell soma and lateral dendrite. Stimulus paradigms resembled those of the behavioral experiments (see METHODS).

First, we compared sound-evoked postsynaptic potentials (PSPs) in response to a 200-Hz, 142-dB sound pip (pulse stimulus) with and without a prepulse stimulus (200 Hz; 136 dB; ISI = 50 ms). A representative example in Fig. 3*A* demonstrates an overall attenuation of the pulse–PSP evoked by the combined prepulse–pulse stimulation (*gray trace*) compared with pulse stimulation alone (*black trace*). Both the control and attenuated pulse–PSP showed the typical waveform for sound-pip responses recorded in the mid-distal lateral dendrite: a short-latency, fast-rising initial component followed by multiple peaks (fast PSP; Szabo et al. 2006). The prepulse appears not to change the timing of these peaks (Figs. 3*A*, *inset* and 4*A*), indicating that although the prepulse stimulus attenuates the overall magnitude of the synaptic response it leaves temporal characteristics of the sensory input unchanged. This differential PPI effect might be important in the context of sensory gating or filtering, since temporal aspects and magnitude of the PSP have been shown to independently encode stimulus frequency and intensity in the M-cell (Szabo et al. 2006).

Another typical feature of sound-pip–evoked PSPs in the M-cell is a slow decaying depolarization PSP (slow PSP; Szabo et al. 2006) that underlies the fast PSP. Such a slow PSP was seen for both prepulse and pulse stimuli (Fig. 3*A*). Hyperpolarizing potentials were not detected following the prepulse, a result consistent with the fact that the reversal potential for inhibitory PSPs and K^+ in the M-cell is close to the resting membrane potential (Faber and Korn 1978; Furukawa 1966).

To quantify and spatially differentiate the prepulse evoked attenuation in the M-cell we recorded sequentially from the dendrite and soma in the same animal and compared peak amplitudes of pulse–PSPs with or without a prepulse on averaged traces (N_T = 10). The results indicated that a prepulse significantly reduced the pulse–PSP peak amplitude in both the dendrite and soma (Fig. 3*B*). The mean PPI effect in the dendrite was 21.3 ± 3.1% (N_A = 8) and in the soma 23.7 ± 2.3% (N_A = 12).

In 2 of 15 animals a pulse stimulus alone regularly evoked APs in the M-cell. In these cases a single AP occurred in about 20% of the trials within 1–2 ms after stimulus onset; i.e., it fired off the initial peak of the evoked PSP (Fig. 3*C*). The low rate of M-cell firing is possibly due to the noted experimental limitation in maximal pulse intensity of 147 dB (see METHODS). Indeed this low M-cell firing rate is consistent with the low escape probability observed in the behavioral experiments with similarly low intensity sound pips (Fig. 1*B*). However, we stress that this limitation did not impair the examination of inhibitory events in the M-cell system evoked by prepulse stimuli (see following text), since prepulse stimuli are subthreshold by definition and their intensities were in the same range as those used in the behavioral experiments.

To test the influence of prepulse intensity and ISI on the synaptic response we varied the prepulse intensity (127–142 dB), while maintaining a constant ISI of 50 ms in one experimental series, and kept the prepulse intensity constant at 136 dB, but altered the prepulse–pulse ISI interval between 50 and 500 ms in another. Pulse intensity was kept constant at 142 dB for both experiments.

Figure 4*A* illustrates the effects of two prepulse intensities on the pulse–PSP recorded in the dendrite, demonstrating a powerful attenuation mediated by the louder prepulse (*red trace*) and a less pronounced attenuation with a weaker prepulse stimulus (*blue trace*). A scatterplot of the normalized pulse–PSP attenuation versus prepulse intensities from five animals suggests the two measures are linearly correlated (R^2 = 0.6; Fig. 4*B*). Moreover, for both prepulse–pulse ISIs we observed attenuations of the pulse–PSP peak compared with controls, i.e., a significant PPI effect (Fig. 4*C*). However, the PPI effect at ISI 500 ms was also significantly less than that at ISI 50 (P = 0.018; N_A = 8).

The prepulse-evoked amplitude attenuation of the synaptic response seems particularly prominent for the initial peaks of the pulse–PSP (Figs. 3*A* and 4*A*). The apparent rapid decay of the PPI effect most likely reflects that it is superimposed on a similar mechanism triggered by the test pulse itself, such as the delayed onset of a feedforward inhibition (see following text). Indeed, previous studies have shown that auditory afferents not only excite the M-cell via a monosynaptic pathway but also stimulate inhibitory interneurons that provide feedforward inhibition to the M-cell via a disynaptic pathway with a delay of 1–2 ms (Faber and Korn 1978; Preuss and Faber 2003). Thus if PPI is due to a postsynaptic inhibitory mechanism, it might be masked by or saturated during the feedforward inhibition evoked by the pulse. However, these considerations also make

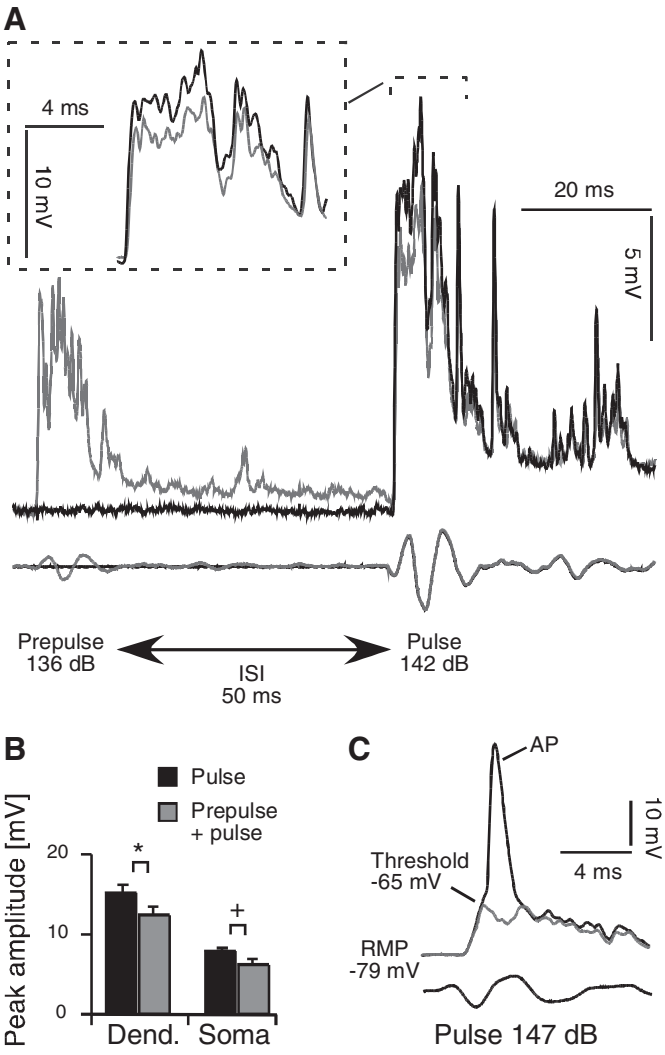

FIG. 3. PPI of synaptic responses in the M-cell. *A*, *top traces*: postsynaptic potentials (PSPs) recorded in the dendrite in response to a pulse without (black) or with (gray) preceding prepulse. *Bottom traces*: hydrophone recordings of the prepulse and pulse stimuli (both 200-Hz sound pips). *Inset*: details of the pulse–PSP at an expanded timescale. *B*: mean peak PSP amplitudes measured in the M-cell lateral dendrite and soma without (black) or with (gray) a preceding prepulse (ISI = 50 ms). Note the PSP amplitude was significantly reduced at both cell loci (*$P = 0.0001$; $N_A = 8$; +$P = 0.008$; $N_A = 12$). *C*, *top traces*: subthreshold (gray) and suprathreshold (black) responses to successive sound pulses recorded in the M-cell soma. *Bottom trace*: hydrophone recordings of the pulse (200 Hz).

it advantageous to characterize the prepulse effect using a test pulse that does not engage the feedforward inhibitory pathway mentioned earlier. This can be achieved by substituting the orthodromic pulse stimulus with a direct stimulation of the M-cell (see following text).

Effects of prepulse stimuli on M-cell membrane properties

One proof of a postsynaptic inhibitory component for the observed attenuation would be the demonstration of a long-lasting influence of the prepulse stimulus on M-cell excitability, such as changes in threshold current or absolute threshold voltage. To quantify these properties in a direct and standardized way we injected a current ramp (20-ms duration; 0–300 nA) into the M-cell via an intrasomatic electrode while simultaneously recording membrane voltage with a second somatic electrode (Fig. 5*A*). A typical experiment involved applying a series of ramp stimuli every 4 s for 2–3 min to assess baseline properties or possible indications for habituation or sensitization, followed by a similar series of ramp stimuli preceded by a prepulse stimulus (Fig. 5*B*). In the latter case, the ramp stimulus was triggered either 50 ms ($N_A = 9$) or 500 ms ($N_A = 6$) after the prepulse, and the mean of all measurements for a given stimulus condition was used for data analysis. Figure 5*A* illustrates the two prominent effects of a prepulse stimulus on the M-cell: an increase in the current necessary to evoke an AP and a substantial reduction (shunt) in amplitude of the evoked AP. Both of these effects were sustained for the duration of prepulse stimulation, although they were more pronounced for ISI 50 than for ISI 500 (Fig. 5*B*, plots 1 and 2 from *top*). In addition, these effects were instantaneous; i.e., they appeared with the first prepulse stimulus and disappear with the first

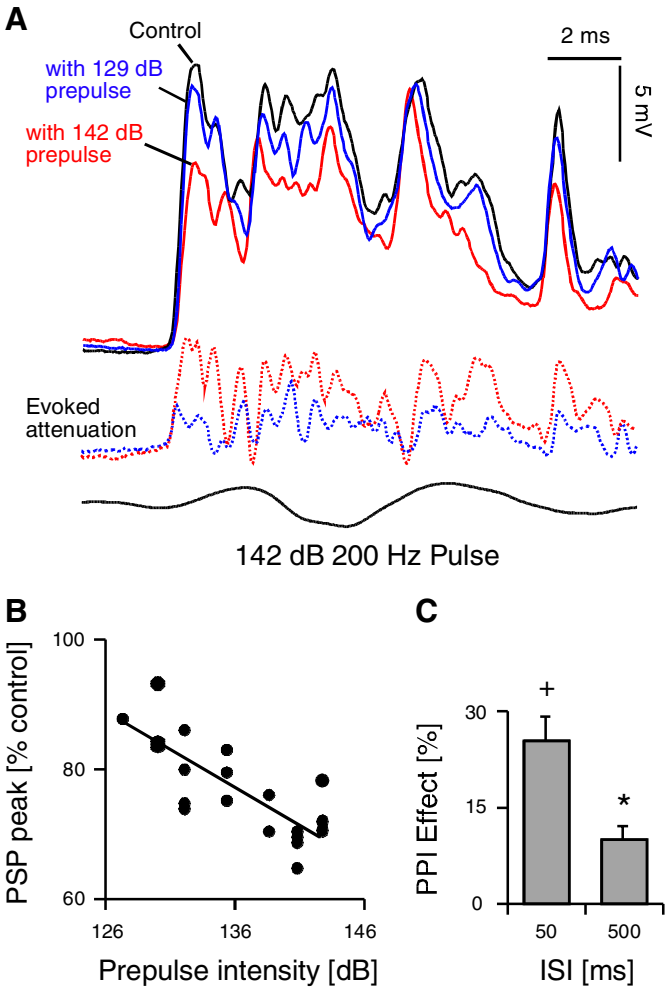

FIG. 4. Physiological characteristics of PPI in the M-cell. *A*, *top traces*: dendritic M-cell PSPs in response to sound pulse without (black) and with a weak (blue) or strong (red) prepulse. *Middle trace*: *blue* and *red dashed traces* show evoked net attenuation (PSP subtraction, control-prepulse) for the 2 prepulse intensities. *Bottom trace*: hydrophone recordings of the pulse stimulus. *B*: influence of prepulse intensity on synaptic PSP. Scatterplot of normalized PSP peak amplitude vs. prepulse intensity from 10 fish fitted with a linear function. Each data point represents the mean of 5 sweeps from individual fish. *C*: effect of ISI on synaptic PPI. Plots of mean PPI effect for indicated ISI times (+$P < 0.0001$, $N_A = 12$; *$P = 0.004$, $N_A = 8$; single-group *t*-test with a test value zero).

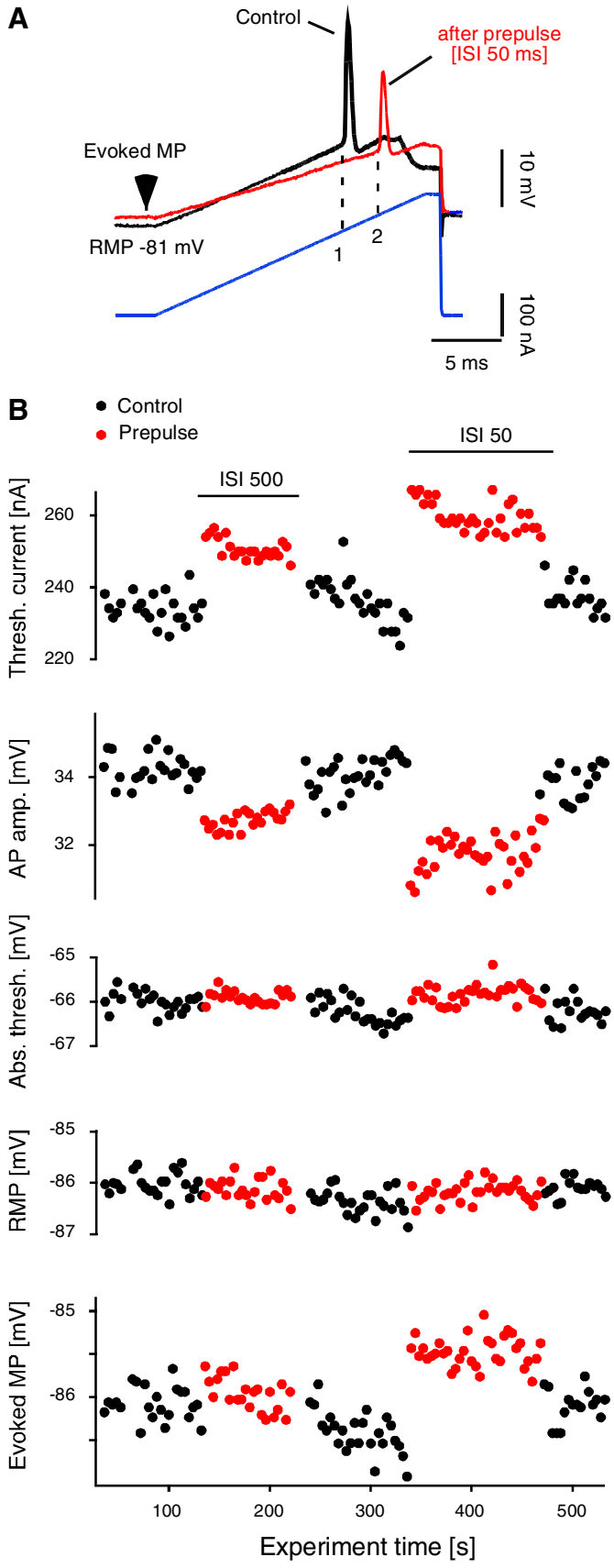

control stimulus. In contrast, absolute M-cell threshold, defined as the difference between resting membrane potential (RMP) and threshold depolarization, was not affected by a prepulse regardless of the ISI used (Fig. 5*B*, *middle plot*). Table 1 shows the quantification and statistical confirmation of these results.

RMP measurements also served as a control for the integrity of the recording and were taken before each stimulus trial (Fig. 5*B*, next to *bottom plot*). Experiments with the RMP value control shifted >4% were not used for data analysis. We also measured the membrane potential 48 or 498 ms after the prepulse to assess how much of the prepulse evoked depolarization (i.e., the previously noted slow PSP of Fig. 3*A*) remained prior to injection of the ramp stimulus.

The results showed this depolarization is small at 48 ms (soma: 0.95 ± 0.02 mV, N_A = 9; dendrite: 1.28 ± 0.07 mV, N_A = 6) and returned essentially to baseline (soma: 0.19 ± 0.05 mV, N_A = 6; dendrite: 0.42 ± 0.04 mV, N_A = 6) at 498 ms (Fig. 5*B*, *bottom plot*).

The dynamic nature of the current-ramp stimulus allowed us to assess other M-cell membrane properties, such as voltage-dependent conductances, over the full range of subthreshold membrane depolarization in a standardized fashion. The voltage–current (*V–I*) plot in Fig. 6*A* shows that the M-cell membrane was linear during the initial depolarization phase, but became increasingly nonlinear with depolarizations >4–5 mV. This nonlinearity may be due to an inward rectifier described previously for the M-cell lateral dendrite (Faber and Korn 1986). In contrast, following a prepulse the M-cell membrane remained linear over the entire depolarization range (Fig. 6*B*). To quantify the prepulse-evoked linearization of the M-cell membrane we applied linear fits to two regions of averaged (N_T = 10) *V–I* plots from individual animals before and after a prepulse and measured the corresponding slopes. Slope region 1 was defined by a 2-ms time interval beginning at the onset of the ramp. Slope region 2 encompassed a similar time window that started 3–4 ms (mean: 3.3 ± 0.2 ms; N_A = 9) before AP threshold (Fig. 6). Table 2 shows the mean values of these slope measurements with and without prepulse for ISI 50 and 500. In controls, we found a 14.4% steeper slope in region 2 compared with that in region 1, a significant difference (P = 0.0035; N_A = 9), supporting the notion of a voltage-dependent nonlinearity in M-cell membrane properties.

Prepulses with lead times of 50 or 500 ms significantly reduced slope 2 by 17.1 ± 2.7% (P = 0.025; N_A = 9) and 6.2 ± 1.7% (P = 0.022; N_A = 6), respectively. In other words, the prepulse diminished the voltage-dependent nonlinearity observed in controls and thus effectively decreased M-cell excitability for moderate depolarizations.

In addition, a comparison of slope 1 before and after a prepulse shows a significant reduction of 13.9 ± 2.9% for ISI

FIG. 5. Postsynaptic effects of prepulse stimuli. *A*, *top 2 traces*: somatic recordings of M-cell membrane voltage without (black) and with (red) a preceding prepulse while injecting a current ramp (blue) with a second somatic electrode. RMP denotes the resting membrane potential before the prepulse. In addition we also measured the evoked membrane potential (MP) following a prepulse just before the start of the ramp (arrowhead). 1 and 2 denote action potential (AP) threshold currents without or with a prepulse, respectively. Note: prepulse increases AP threshold current and reduces AP amplitude but leaves absolute threshold voltage unchanged. *B*: consecutive measurements of indicated membrane properties during a representative experiment.

TABLE 1. *Effect of prepulse on M-cell membrane properties*

ISI	Membrane Property	Control	PPI	PPI Effect	*P* Values
50 (N_A = 9)	AP amp., mV	41.5 ± 2.5	38.50 ± 3.2	8.37 ± 2.89	**P* = 0.012
	Abs. thresh., mV	−65.6 ± 1.0	−65.4 ± 1.1	0.21 ± 0.21	*P* = 0.354
	Thresh. current, nA	174.7 ± 15.7	190.1 ± 18.2	8.30 ± 1.47	**P* = 0.001
500 (N_A = 6)	AP amp., mV	44.2 ± 3.6	42.96 ± 3.4	2.80 ± 0.79	**P* = 0.027
	Abs. thresh., mV	−65.8 ± 1.4	−65.7 ± 1.5	0.09 ± 0.31	*P* = 0.742
	Thresh. current, nA	166.7 ± 18.8	175.2 ± 20.7	4.74 ± 1.5	**P* = 0.036

Values are means ± SE. Measurements (10–15 sweeps) from individual fish for action potential amplitude (AP amp.), absolute threshold (Abs. thresh.), and threshold current (Thresh. current) for controls and ISI 50 and 500 ms were averaged and the resulting means were compared using paired *t*-tests.

50 (P = 0.025; N_A = 9) and a smaller, 3.7 ± 2.2%, reduction for ISI 500. However, the latter did not reach the level of significance (P = 0.19; N_A = 6). The close proximity of the current and voltage electrode in the soma allows one to consider slope 1 (i.e., the slope that reflects the linear portion of the *V–I* plot) a direct representation of M-cell input resistance. Thus the reduction of slope 1 for ISI 50 indicates a decrease in M-cell input resistance that is less pronounced or absent at longer prepulse lead times. Taken together, the ramp experiments demonstrate that a prepulse evokes a long-lasting decrease in M-cell excitability, which presumably involves two postsynaptic inhibitory mechanisms operating on different timescales.

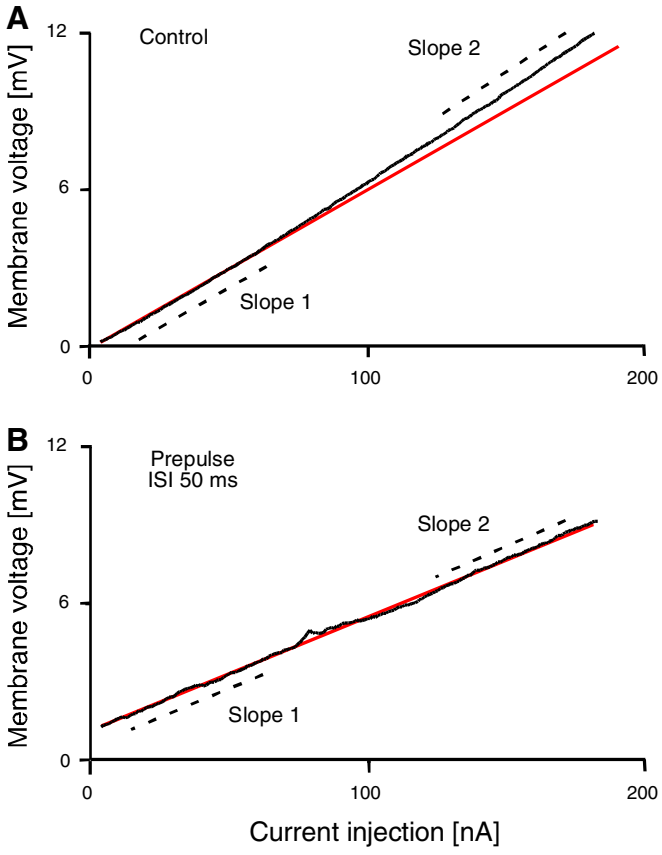

FIG. 6. Effect of prepulse on nonlinear M-cell membrane properties. *Voltage–current* (*V–I*) *traces* (average of 10 consecutive sweeps) show M-cell membrane depolarizations (*black traces*) during a current ramp without (*A*) or with (*B*) a prepulse. The depicted range covers the evoked depolarization to about 2 mV below AP threshold. *Red traces* in *A* and *B* indicate linear fits to the initial part of the *V–I* plot (i.e., to the Slope 1 region). Slope 2 indicates the region where a second linear fit was applied to the top part of the *V–I* plot (fit not shown in graph). Note the M-cell membrane shows a voltage-dependent nonlinearity for depolarizations >4 mV (*A*) that is eliminated after a prepulse (*B*).

The decreased input resistance at resting potential could be due to postsynaptic inhibition, and a well-established method to quantify this inhibition in the M-cell is to measure the amplitude reduction of an antidromically evoked test AP by a preceding conditioning stimulus (Fig. 7*A*; Faber and Korn 1978; Furukawa 1966). In short, such a reduction has been shown to be proportional to an increase in membrane conductance (i.e., to an inhibitory shunt). We therefore used a prepulse as the conditioning stimulus that preceded the test antidromic AP with ISIs ranging from 20 to 550 ms to analyze the magnitude and time course of the evoked feedforward inhibition at the M-cell soma and dendrite. For each ISI, averages of five test AP amplitude measurements were taken with or without a prepulse to calculate the corresponding inhibitory shunt at that time. Figure 7*B* presents the results of four experiments as a combined scatterplot and shows that overall inhibition was more pronounced in the dendrite. For ISIs ranging from 40 to 60 ms the mean shunt was 17.6 ± 1.7% in the dendrite and 7.9 ± 0.6% in the soma (P < 0.009, unpaired *t*-test; N_A = 4). ISIs ranging from 100 to 200 ms evoked a mean shunt of 12.7 ± 3.4% in the dendrite and 1.7 ± 0.3% in the soma (P < 0.04, unpaired *t*-test; N_A = 4).

The time course of dendritic inhibition showed a fast initial decay for ISIs ranging from 20 to 40 ms followed by a slow decaying second component, with inhibition still present at 500 ms (Fig. 7*B*). In contrast, somatic inhibition showed a rather continuous decay, which was almost gone by 200 ms (i.e., it apparently lacks a second component). To substantiate these differences in timecourse we applied single- and double-exponential fits to both data sets in Igor Pro, and found that dendritic inhibition was best represented with a double-exponential function with a tau (τ) of 17.6 ms for the initial component and a τ of 694 ms for the second component. In contrast, somatic inhibition was best fit with a single exponential with τ of 50.7 ms.

TABLE 2. *Effect of prepulse on subthreshold M-cell membrane depolarization*

ISI	Membrane Property	Control, kΩ	PPI, kΩ
50 (N_A = 9)	*V–I* slope 1	97 ± 15	83 ± 11
	V–I slope 2	111 ± 17	90 ± 10
500 (N_A = 6)	*V–I* slope 1	90 ± 7	87 ± 8
	V–I slope 2	102 ± 9	95 ± 8

Values are means ± SE. Linear fits were applied to regions 1 and 2 in averaged *V–I* plots (see Fig. 6) for controls and ISI 50 and 500 ms and used to calculate the corresponding mean slopes 1 and 2.

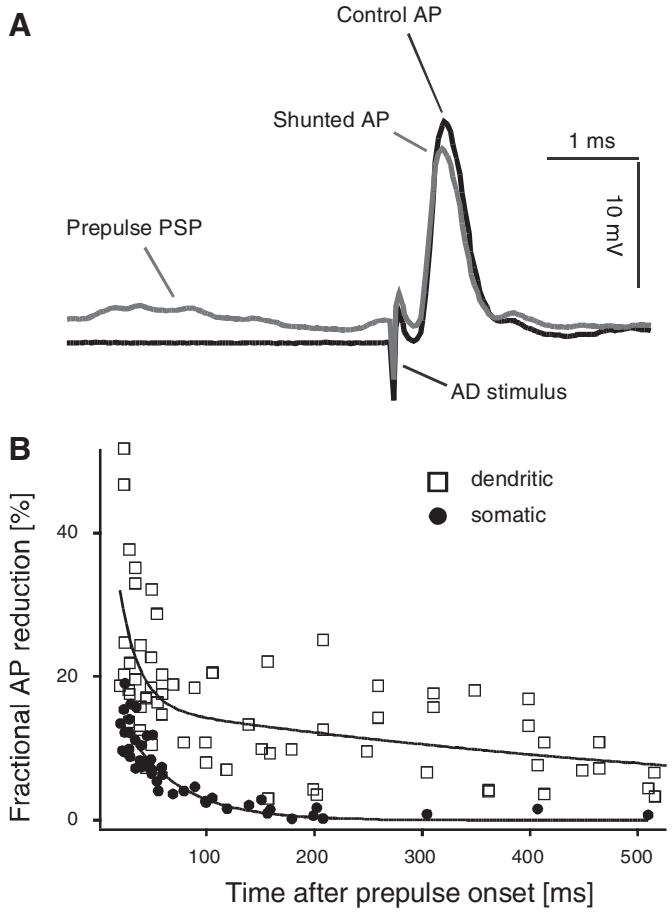

FIG. 7. Dendritic vs. somatic inhibition in the M-cell. *A*: superimposed intrasomatic recordings of the antidromically (AD)-evoked test AP without (black) or with (gray) a preceding prepulse. Note: the prepulse evokes a fractional reduction of the AP (i.e., an inhibitory shunt). *B*: scatterplot shows the magnitude of the inhibitory shunt measured at varying prepulse lead times in the lateral dendrite and soma ($N_A = 4$). Decays of the dendritic and somatic shunts were fitted with double- and single-exponential functions, respectively. Individual data points in *B* are averages of 5 sweeps.

DISCUSSION

In this study, we examined the effects of an auditory prepulse–pulse stimulus paradigm on the goldfish startle escape and the underlying physiological response in the cell triggering this behavior: the M-cell. The main behavioral results are *1*) that a prepulse–pulse paradigm with stimulus characteristics similar to those used for PPI in mammals reliably attenuates escape probability in goldfish. This finding complements similar results reported recently for zebrafish (Burgess and Granato 2007). *2*) PPI increases with prepulse intensity, but seems less affected by the prepulse lead time within the tested range.

The electrophysiological results demonstrate the following. *1*) An auditory prepulse significantly attenuates the synaptic response to a subsequent sound pulse in the M-cell soma and lateral dendrite, thus providing a cellular correlate for PPI with physiological stimuli. *2*) A prepulse stimulus induces a long-lasting decrease of M-cell excitability by decreasing its input resistance and by reducing the depolarizing effect of a M-cell membrane nonlinearity. The latter results imply that postsynaptic changes in the M-cell system correlate to behavioral PPI and are, to our knowledge, the first demonstration of such a mechanism in the vertebrate auditory startle pathway. *3*) A comparison of the time course and magnitude of postsynaptic inhibition evoked by a prepulse in the M-cell dendrite and soma revealed a disproportionately larger inhibitory shunt in the dendrite. This finding is consistent with the notion that the cellular mechanism(s) underlying PPI is (are) mediated primarily at the M-cell lateral dendrite.

PPI in the M-cell system

The electrophysiology results show that an auditory prepulse–pulse paradigm significantly attenuates postsynaptic potential responses (PSPs) in the M-cell. The magnitude of this attenuation was proportional to prepulse intensity over the tested range and was maximal at a prepulse lead time of 50 ms. In addition, there was still a significant attenuation of the PSP at a prepulse lead time of 500 ms. Interestingly, PPIs of sound-evoked PSPs and spike firing rates have similar dependencies on prepulse amplitude and lead time in giant neurons (PnC neurons) in the rat caudal pontine reticular nucleus (Carlson and Willott 1998; Lingenhöhl and Friauf 1994).

Both M-cells and PnC neurons receive direct VIIIth nerve auditory input with a delay of 1–2 ms and activate spinal motor neurons within 3–4 ms after startle stimulus onset (Davis et al. 1982; Eaton et al. 1981; Lingenhöhl and Friauf 1994; Szabo et al. 2006; Yeomans et al. 1989; Zottolli 1977). These physiological and functional similarities provide, we believe, a strong tie between PPI in both systems. The central role these neurons play in mediating startle (Korn and Faber 1996) makes them likely sites for inhibitory mechanism(s) underlying PPI. For PnC neurons this notion is supported by neurophysiological and pharmacological experiments (Bosch and Schmid 2006; Carlson and Willott 1998; Fendt and Koch 1999; Lingenhöhl and Friauf 1992). The present study adds to this idea by directly demonstrating postsynaptic mechanisms for a PPI-type phenomenon in the M-cell (see following text).

In teleosts, the role of a sensorimotor integrator is filled by a pair of large neurons, the M-cells, rather than being distributed within a small population of PnC neurons (Lingenhöhl and Friauf 1992, 1994; Nodal and Lüpez 2003). This structural disparity requires using different behavioral measures of PPI in the two systems. As discussed previously by Burgess and Granato (2007), PPI in rats is characterized and measured as a graded attenuation of the startle magnitude, which presumably reflects a prepulse-induced depression in the firing rates of numerous PnC neurons. In contrast, PPI in fish either does or does not block initiation of the short-latency startle, related to whether one M-cell does or does not reach threshold and fires a single action potential. This binary output condition is because a single M-axon AP precedes each C-start startle (Eaton et al. 1981; Weiss et al. 2006; Zottoli 1977), and it underlies the rationale for quantifying PPI in fish by a change in C-start probability.

Our behavioral results demonstrate maximum C-start probabilities of <0.8 (Fig. 1*B*), reflecting the fact that the low input resistance M-cell ($\sim$94 kΩ; *V–I* slope 1 in Fig. 6 and Table 2) is a high-threshold neuron. In other words, it is hard to bring the cell to the firing level and one might not expect that the sound-evoked PSPs rise well beyond threshold. Thus even a relatively small decrease in M-cell excitability at an ISI of 500 ms (Table 1) might still be sufficiently large to suppress the generation of an M-cell AP (and the expression of the all-or-

none behavior). This might explain why the magnitude of behavioral PPI decreased only slightly at longer ISIs, although the electrophysiology results showed an appreciably smaller PPI effect at an ISI of 500 ms compared with 50 ms. In both ISIs the attenuated PSPs may have been only large enough to evoke escapes in about 15 to 20% of the trials (~75% PPI effect in Fig. 2*C*).

As noted, behavioral PPI of M-cell–mediated acoustic startle has been described for zebrafish larvae and young adults. The time course of this PPI is developmentally dependent, with a maximum at 300 or 50 ms and lasting for 3–4 s or 800 ms in the larvae and adult, respectively (Burgess and Granato 2007). These findings are comparable to our results (Fig. 2*C*), although one has to consider that the nearly 8–10°C lower ambient temperature in our study may produce a slightly longer lasting inhibitory PPI effect (Preuss and Faber 2003). Notably, mammalian PPI shows its maximum also between 50 and 200 ms and lasts ≤1 s (Diederich and Koch 2005; Hoffman and Ison 1980; Winslow et al. 2002). Moreover, the zebrafish study also emphasized another similarity to mammalian PPI, since PPI is modulated by dopamine in both species (Burgess and Granato 2007).

Taken together these findings suggest that PPI in fish and mammals indeed share many properties at the physiological and behavioral levels.

Postsynaptic mechanisms of PPI in the M-cell

Both the increase in threshold current and the inhibitory shunt of the AP seen with somatic current injections are consistent and direct indicators of a significant postsynaptic component underlying PPI in the M-cell. Specifically, our physiological results implicate an inhibitory mechanism localized at the lateral dendrite. We conclude this from experiments using a sound prepulse as a conditioning stimulus, but two different responses to assess inhibition in the soma and dendrite: *1*) the PSP evoked by a sound pulse, (i.e., a dendritic, orthodromic source) and *2*) an antidromically evoked AP (i.e., a somatic source). Spread of both responses along the soma-dendritic M-cell membrane is governed by passive cable properties (Furukawa 1966; Preuss and Faber 2003; Szabo et al. 2006). A comparison of the PPI effect at the soma versus the dendrite showed a similar PSP reduction at both cell locations of about 23–25%. However, although the antidromically evoked AP was shunted by 22% in the dendrite, it was decreased only about 10% in the soma. These results are consistent with dendritic inhibition because a primarily somatic inhibition would rather produce a comparable shunt of the antidromic AP at both recording sites, but a relatively stronger PSP reduction in the soma (Furukawa 1966).

Our experiments were designed to elucidate postsynaptic inhibitory mechanisms of PPI in the M-cell system, and we cannot exclude the possibility that part of the observed PSP attenuation was mediated by a presynaptic mechanism, e.g., at the level of the VIIIth nerve fibers. This notion has to be considered critically, given the evidence provided by the elegant study by Frost and colleagues (2003), which identified pre- and postsynaptic mechanisms underlying PPI in a marine mollusk. However, is seems that the increase in excitability of the postsynaptic M-cell membrane following a prepulse can account for most of the observed attenuation of the synaptic response (see following text).

We believe these results are an important step toward understanding the cellular mechanisms of PPI because they add to the current view with respect to where PPI is mediated in the elementary auditory startle pathway of vertebrates. Indeed, although physiological studies in PnC neurons in rats rather emphasize a presynaptic component for PPI, an alternative postsynaptic mechanism has not been excluded (Bosch and Schmid 2006; Lingenhöhl and Friauf 1994).

The pivotal role of an M-cell AP in the startle escape makes it clear that its generation has to be a stringently controlled yet reliable process. The latter is reflected in specific M-cell membrane properties such as the voltage-dependent nonlinearity observed in the current-ramp experiments for membrane depolarization above 4–5 mV in the M-cell soma (Fig. 6*A*). Especially in a high-threshold neuron with relatively low input resistance such a nonlinearity is thought to enhance the likelihood of generating an AP preferably to massive and synchronous excitatory inputs (Faber and Korn 1986). Our experiments demonstrate that a prepulse stimulus significantly reduced this membrane nonlinearity [i.e., slope 2 of the *V–I* plots (Fig. 6)] and thus effectively decreased M-cell excitability. This conclusion is valid regardless of whether the increased slope in region 2 in control conditions reflects an increased membrane resistance or a subthreshold depolarizing inward current.

Prepulse stimuli also significantly decreased the M-cell input resistance in the region of the resting potential. This effect was demonstrated by a change of slope 1 (see *V–I* plots in Fig. 6 and Table 2) as well as in the sizeable inhibitory shunt of the orthodromically and antidromically evoked AP (Figs. 5*A* and 7*B*; Table 1). Taken together these results imply at least two different postsynaptic inhibitory mechanisms that increase M-cell excitability during PPI. The differential effect on input resistance between ISI 50 and 500 ms—i.e., the fact that slope 1 was significantly reduced only at shorter prepulse lead times—further supports this notion.

Multiple temporally and spatially distinct mechanisms associated with PPI have been proposed previously in another model system (Frost et al. 2003; Nussbaum and Contreras 2004) and our results are consistent with this idea. Thus a general scenario might be that PPI is mediated by several mechanisms working in concert and/or sequentially at the pre- and postsynaptic membrane.

In humans, PPI is used to detect information processing deficits in schizophrenic patients (Braff et al. 2001; Ludewig et al. 2003) as well as in other neurological disorders (Swerdlow et al. 1993, 1995). Thus we believe the present characterization of PPI in the M-cell system, including its underlying cellular mechanisms, increases our understanding of PPI in general and could add to its value as a research tool for neurological and neuropsychiatric disorders.

ACKNOWLEDGMENTS

We thank D. S. Faber for helpful experimental suggestions and comments on the manuscript and P. E. Osei-Bonsu, K. Fisher, and M. Volaski for technical assistance. We also thank the departmental behavioral core for assistance with statistical analysis.

REFERENCES

Bosch D, Schmid S. Activation of muscarinic cholinergic receptors inhibits giant neurons in the caudal pontine reticular nucleus. *Eur J Neurosci* 24: 1967–1975, 2006.

Braff DL, Geyer MA, Swerdlow NR. Human studies of prepulse inhibition of startle: normal subjects, patient groups, and pharmacological studies. *Psychopharmacology* 156: 234–258, 2001.

Burgess HA, Granato M. Sensorimotor gating in larval zebrafish. *J Neurosci* 27: 4984–4994, 2007.

Carlson S, Willott JF. Caudal pontine reticular formation of C57BL/6J mice: responses to startle stimuli, inhibition by tones, and plasticity. *J Neurophysiol* 79: 2603–2614, 1998.

Casagrand JL, Guzik AL, Eaton RC. Mauthner and reticulospinal responses to the onset of acoustic pressure and acceleration stimuli. *J Neurophysiol* 82: 1422–1437, 1999.

Davis M, Gendelman DS, Tischler MD, Gendelman PM. A primary acoustic startle circuit: lesion and stimulation studies. *J Neurosci* 2: 791–805, 1982.

Diederich K, Koch M. Role of the pedunculopontine tegmental nucleus in sensorimotor gating and reward-related behavior in rats. *Psychopharmacology* 179: 402–408, 2005.

Eaton RC. *Neural Mechanisms of Startle Behavior.* New York: Plenum Press, 1984.

Eaton RC, DiDomenico R, Nissanov J. Role of the Mauthner cell in sensorimotor integration by the brain stem escape network. *Brain Behav Evol* 37: 272–285, 1991.

Eaton RC, Lavender WA, Wieland CM. Identification of Mauthner-initiated patterns in goldfish: evidence from simultaneous cinematography and electrophysiology. *J Comp Physiol A Neuroethol Sens Neural Behav Physiol* 144: 521–531, 1981.

Faber DS, Fetcho JR, Korn H. Neuronal networks underlying the escape response in goldfish. General implications of motor control. *Ann NY Acad Sci* 563: 11–33, 1989.

Faber DS, Korn H. Electrophysiology of the Mauthner cell: basic properties, synaptic mechanisms and associated networks. In: *Neurobiology of the Mauthner Cell*, edited by Faber DS, Korn H. New York: Raven Press, 1978, p. 47–131.

Faber DS, Korn H. Instantaneous inward rectification in the Mauthner cell: a postsynaptic booster for excitatory inputs. *Neuroscience* 19: 1037–1043, 1986.

Faber DS, Triller A, Korn H. Structural correlates of recurrent collateral interneurons producing both electrical and chemical inhibitions of the Mauthner cell. *Proc R Soc Lond B Biol Sci* 202: 533–538, 1978.

Fay RR. The goldfish ear codes the axis of particle motion in three dimensions. *Science* 225: 951–953, 1984.

Fendt M, Koch M. Cholinergic modulation of the acoustic startle response in the caudal pontine reticular nucleus of the rat. *Eur J Pharmacol* 370: 101–107, 1999.

Fendt M, Li L, Yeomans JS. Brain stem circuits mediating prepulse inhibition of the startle reflex. *Psychopharmacology* 156: 216–224, 2001.

Frost WN, Tian LM, Hoppe TA, Mongeluzi DL, Wang J. A cellular mechanism for prepulse inhibition. *Neuron* 40: 991–1001, 2003.

Furukawa T. Synaptic interaction at the Mauthner cell of goldfish. *Prog Brain Res* 21: 44–70, 1966.

Furukawa T, Ishii Y. Neurophysiological studies on hearing in goldfish. *J Neurophysiol* 30: 1377–1403, 1967.

Graham FK. The more or less startling effects of weak prestimulation. *Psychophysiology* 12: 238–248, 1975.

Grillon C, Baas J. A review of the modulation of the startle reflex by affective states and its application in psychiatry. *Clin Neurophysiol* 114: 1557–1579, 2003.

Hoffman HS, Ison JR. Reflex modification in the domain of startle: I. Some empirical findings and their implications for how the nervous system processes sensory input. *Psychol Rev* 87: 175–189, 1980.

Koch M. The neurobiology of startle. *Prog Neurobiol* 59: 107–128, 1999.

Korn H, Faber DS. Escape behavior: brainstem and spinal cord circuitry and function. *Curr Opin Neurobiol* 6: 826–832, 1996.

Korn H, Faber DS. The Mauthner cell half a century later: a neurobiological model for decision-making. *Neuron* 47: 13–28, 2005.

Lee Y, Lopez DE, Meloni EG, Davis M. A primary acoustic startle pathway: obligatory role of cochlear root neurons and the nucleus reticularis pontis caudalis. *J Neurosci* 16: 3775–3789, 1996.

Lingenhöhl K, Friauf E. Giant neurons in the caudal pontine reticular formation receive short latency acoustic input: an intracellular recording and HRP-study in the rat. *J Comp Neurol* 325: 473–492, 1992.

Lingenhöhl K, Friauf E. Giant neurons in the rat reticular formation: a sensorimotor interface in the elementary acoustic startle circuit? *J Neurosci* 14: 1176–1194, 1994.

Liu KS, Fetcho JR. Laser ablations reveal functional relationships of segmental hindbrain neurons in zebrafish. *Neuron* 23: 325–335, 1999.

Ludewig K, Geyer MA. Deficits in prepulse inhibition and habituation in never-medicated, first-episode schizophrenia. *Biol Psychiatry* 54: 121–128, 2003.

Mongeluzi DL, Hoppe TA, Frost WN. Prepulse inhibition of the *Tritonia* escape swim. *J Neurosci* 18: 8467–8472, 1998.

Nodal FR, Lüpez DE. Direct input from cochlear root neurons to pontine reticulospinal neurons in albino rat. *J Comp Neurol* 460: 80–93, 2003.

Nusbaum MP, Contreras D. Sensorimotor gating: startle submits presynaptic inhibition. *Curr Biol* 14: R247–R249, 2004.

Palmer LM, Mensinger AF. Effect of anesthetic tricaine (MS-222) on nerve activity in the anterior lateral line of the oyster toadfish, *Opsanus tau.* *J Neurophysiol* 92: 1034–1041, 2004.

Popper AN, Fay RR. The auditory periphery in fishes. In: *Comparative Hearing: Fish and Amphibians*, edited by Fay RR, Popper AN. New York: Springer-Verlag, 1999, p. 43–100.

Preuss T, Faber DS. Central cellular mechanisms underlying temperature dependent changes in the goldfish startle-escape behavior. *J Neurosci* 23: 5617–5626, 2003.

Swerdlow NR, Benbow CH, Zisook S, Geyer MA, Braff DL. A preliminary assessment of sensorimotor gating in patients with obsessive compulsive disorder. *Biol Psychiatry* 33: 298–301, 1993.

Swerdlow NR, Geyer MA. Using an animal model of deficient sensorimotor gating to study the pathophysiology and new treatments of schizophrenia. *Schizophr Bull* 24: 285–301, 1998.

Swerdlow NR, Geyer MA, Braff DL. Neural circuit regulation of prepulse inhibition of startle in the rat: current knowledge and future challenges. *Psychopharmacology* 156: 194–215, 2001.

Swerdlow NR, Paulsen J, Braff DL, Butters N, Geyer MA, Swenson MR. Impaired prepulse inhibition of acoustic and tactile startle response in patients with Huntington's disease. *J Neurol Neurosurg Psychiatry* 58: 192–200, 1995.

Szabo TM, McCormick CA, Faber DS. Otolith endorgan input to the Mauthner neuron in the goldfish. *J Comp Neurol* 505: 511–525, 2007.

Szabo TM, Weiss SA, Faber DS, Preuss T. Representation of auditory signals in the M-cell: role of electrical synapses. *J Neurophysiol* 95: 2617–2629, 2006.

Weiss SA, Zottoli SJ, Do SC, Faber DS, Preuss T. Correlation of C-start behaviors with neural activity recorded from the hindbrain in free-swimming goldfish (*Carassius auratus*). *J Exp Biol* 209: 4788–4801, 2006.

Winslow JT, Parr LA, Davis M. Acoustic startle, prepulse inhibition, and fear-potentiated startle measured in rhesus monkeys. *Biol Psychiatry* 51: 859–866, 2002.

Yeomans JS, Frankland PW. The acoustic startle reflex: neurons and connections. *Brain Res Rev* 21: 301–314, 1996.

Yeomans JS, Rosen JB, Barbeau J, Davis M. Double-pulse stimulation of the startle-like responses in rats: refractory periods and temporal summation. *Brain Res* 486: 147–158, 1989.

Zhang J, Forkstam C, Engel JA, Svennson L. Role of dopamine in prepulse inhibition of acoustic startle. *Psychopharmacology* 149: 181–188, 2000.

Zottoli SJ. Correlation of the startle reflex and Mauthner cell auditory responses in unrestrained goldfish. *J Exp Biol* 66: 243–254, 1977.

Zottoli SJ, Newman BC, Rieff HI, Winters DC. Decrease in occurrence of fast startle responses after selective Mauthner cell ablation in goldfish. *J Comp Physiol A Sens Neural Behav Physiol* 184: 207–218, 1999.